Multiphoton microscopy study of the morphological and quantity changes of collagen and elastic fiber components in keloid disease

Jianxin Chen,[a] Shuangmu Zhuo,[a] Xingshan Jiang,[a] Xiaoqin Zhu,[a] Liqin Zheng,[a] Shusen Xie,[a] Bifang Lin,[b] and Haishan Zeng[c]

[a]Fujian Normal University, Institute of Laser and Optoelectronics Technology, Fujian Provincial Key Laboratory for Photonics Technology, Key Laboratory of OptoElectronic Science and Technology for Medicine of Ministry of Education, Fuzhou 350007, China
[b]Fuzhou First Hospital, Department of Dermatology, Fuzhou 350009, China
[c]British Columbia Cancer Agency Research Centre, Cancer Imaging Department, Vancouver, BC, V5Z 1L3, Canada

Abstract. Multiphoton microscopy was used to study the extracellular matrix of keloid at the molecular level without tissue fixation and staining. Direct imaging of collagen and elastin was achieved by second harmonic generation and two-photon excited fluorescence, respectively. The morphology and quantity of collagen and elastin in keloid were characterized and quantitatively analyzed in comparison to normal skin. The study demonstrated that in keloid, collagen content increased in both the upper dermis and the deep dermis, while elastin mostly showed up in the deep dermis and its quantity is higher compared to normal skin. This suggests the possibility that abnormal fibroblasts synthesized an excessive amount of collagen and elastin at the beginning of keloid formation, corresponding to the observed deep dermis, while after a certain time point, the abnormal fibroblast produced mostly collagen, corresponding to the observed upper dermis. The morphology of collagen and elastin in keloid was disrupted and presented different variations. In the deep dermis, elastic fibers showed node structure, while collagen showed obviously regular gaps between adjacent bundles. In the upper dermis, collagen bundles aligned in a preferred direction, while elastin showed as sparse irregular granules. This new molecular information provided fresh insight about the development process of keloid.
[DOI: 10.1117/1.3569617]

Keywords: multiphoton microscopy; second harmonic generation; two-photon excited fluorescence; keloid; collagen; elastin; molecular information.

Paper 10625R received Nov. 24, 2010; revised manuscript received Feb. 22, 2011; accepted for publication Mar. 2, 2011; published online May 2, 2011.

1 Introduction

Human keloids are characterized by the deposition of excessive extracellualar matrix components produced by abnormal fibroblasts (the so-called keloid-derived fibroblasts) in response to cutaneous injury. They occur at areas of cutaneous injury that do not regress or contract, and continue to grow and extend beyond the confine of the original wound.[1,2] They can lead to pain, pruitus, deformity, or limiting joint mobility, and considerable cosmetic defects.[2–4] Unfortunately, there is no effective treatment modality that has been established for human keloids.[2,5] There are very high recurrence rates after surgical removal of keloids. It is becoming increasingly obvious that limitation of existing treatments just highlights the urgency on achieving better understanding of this disease at the molecular level.

Keloids are unique to humans. There is no animal model available for study of the molecular progress of keloids. Existing studies are based on histological method, electron microscopy, and immunohistochemical techniques.[4,6,7] These methods usually involve fixation, staining, and dehydration of biopsied tissue specimens, and the native morphology of collagen and elastin are altered.

The most significant advantage of multiphoton microscopy based on two-photon excited fluorescence (TPEF) and second harmonic generation (SHG) imaging is its capability of observing non-fixed, unstained tissue samples. It also has the potential of perform noninvasive *in vivo* measurements directly on a patient. Because collagen in the skin dermis can easily produce a SHG signal and elastin are more effective in generating TPEF, multiphoton microscopy has found widespread applications in dermatology for studying cutaneous collagen and elastin. For example, this technique has been used to study normal skin, assess skin aging and photoaging, and diagnose basal cell carcinoma.[8–11] Recently, it has become a new technology for studying wound healing[12–14] and for differentiating keloid and hypertrophic scars from normal skin.[3,15,16] In this study, morphology and quantities of collagen and elastin in human keloid tissues were characterized, quantitatively analyzed, and compared with normal skin using multiphoton microscopy. The results provided new molecular information useful for understanding the development process of keloid.

Address all correspondence to Jianxin Chen, Fujian Normal University, Institute of Laser & Optoelectronic Technology, No. 8 Shangshan Rd, Fuzhou, Fujian 350007, China or Haishan Zeng, British Columbia Cancer Agency Research Center, Cancer Imaging Department, 675 West 10th Avenue, Vancouver, BC, V5Z IL3 Canada.

1083-3668/2011/16(5)/051305/6/$25.00 © 2011 SPIE

2 Materials and Methods

2.1 *Ex-vivo Human Keloid Specimens*

Five keloid samples were obtained from 5 patients (age 32 to 55 years) undergoing reconstructive surgical procedures. Five normal skin samples were collected during aesthetic plastic surgery from 5 healthy subjects aged 30 to 58 years old. Informed consent was obtained from every patient who participated in the study. We strictly conformed to the institutional rules governing clinical investigation of human subjects in biomedical research. Immediately after being excised from patients, tissue samples were snap-frozen and kept in liquid nitrogen [at atmospheric pressure, liquid nitrogen boiling point is at 77 K (−196°C)] until use in order to avoid protein denaturization and preserve native morphology. The tissue sections for multiphoton microscopic imaging were cut into 120-μm thickness and sandwiched between the microscope slide and cover glass. The sample was imaged with the cover glass facing the microscopic objective.

2.2 *Multiphoton Microscopy Imaging System*

The multiphoton microscopy system used in this work has been described previously.[8,15] The system is a high-throughput scanning inverted Axiovert 200 microscope (Zeiss LSM 510 META) equipped with a mode-locked femtosecond Ti:sapphire laser (Coherent Mira 900-F). For high-resolution imaging, a high-numerical-aperture, oil immersion objective (Plan-Apochromat 63×, N.A.1.4, Zeiss) was employed in all experiments. In the multichannel mode, the backward SHG and TPEF signals from tissue samples were collected by the META detector with eight independent channels. In this work, two different channels were selected to obtain the high contrast images of collagen and elastin in the dermis of keloid scar and normal skin. One channel is corresponding to the wavelength range of 398 to 409 nm to show the microstructure of collagen using SHG signals, whereas another channel covered the wavelength range from 430 to 697 nm in order to present the morphology of elastin using TPEF signals when an excitation wavelength of 810 nm was used. In order to increase the contrast of the SHG/TPEF image, the collagen images are color-coded in green and elastin images are color-coded in red. All images have a 12-bit pixel depth. The images were obtained at 2.56-μs per pixel. Under the transmission mode, a large field mosaic image from the epidermis to the dermis of keloid scar tissue was acquired to better illustrate the multiphoton microscopic imaging results.

2.3 *Quantitative Analysis of Collagen and Elastin Volume Density*

In order to calculate collagen and elastin volume density, sequential 2-D images were taken at intervals of 2 μm to a final depth of 30 μm, resulting in a total of 15 images per tissue sample. Then this stack of two-dimensional images were used to reconstruct a 3-D multiphoton microscopic image of the collagen and elastin within the tissue specimen. Quantitative analysis of collagen and elastin volume density was performed using the following method. The pixel numbers of collagen SHG image, elastin TPEF image, and the total pixel number of the whole area within each of the 15 sequential 2-D images were defined as A_i, B_i, and C (the total pixel of each 2-D image is identical), respectively. C is usually larger than $A_i + B_i$. Then the volume density of collagen or elastin was calculated by using the following formula: $\sum_{i=1}^{i=15} A_i/15C$ and $\sum_{i=1}^{i=15} B_i/15C$, respectively. In this nomenclature, the higher ratio value indicates that the quantity of collagen or elastin is higher. All data in this paper are presented as a mean value followed by its standard deviation (mean ± SD).

3 Results

3.1 *Large Field Image of Keloid Tissue with Transmission Mode Microscopy*

The transmission mode microscopy is based on optical density recognition of the detected transmitted light from the sample to be visualized. The difference of tissue specimen component can be delineated in sub-millimeter size.[17] The cross dimension from the top of the epidermis to the bottom of the dermis of the keloid tissues examined in this study was several millimeters. To better illustrate the following multiphoton microscopy imaging results of keloid scar, the transmission microscopy image of keloid tissue was recorded. Figure 1 shows a representative transmission mode image of a keloid scar (from a 51-year-old patient) with an average thickness of 7.49 ± 0.21 mm. This is a mosaic of 154 individual 925×925 μm^2 size transmission images obtained by scanning the microscope sample stage. There are two boundaries (the white lines approximate indicate their corresponding positions). The first boundary is corresponding to the epidermal-dermal junction that reflected the differences on the optical densities between epidermis and dermis: the epidermis consists mostly of keratin and epithelial cells, while the dermis is dominated by collagen and/or elastin. The second boundary is within the dermis, representing a very interesting result. It indicates that there are obviously differences on the molecular compositions and/or morphological structures that resulted in different absorption or scattering properties in two sides of this boundary. It will be interesting to see if multiphoton microscopy can reveal these differences. For convenient discussion, we call the dermal part between the epidermal-dermal junction and the

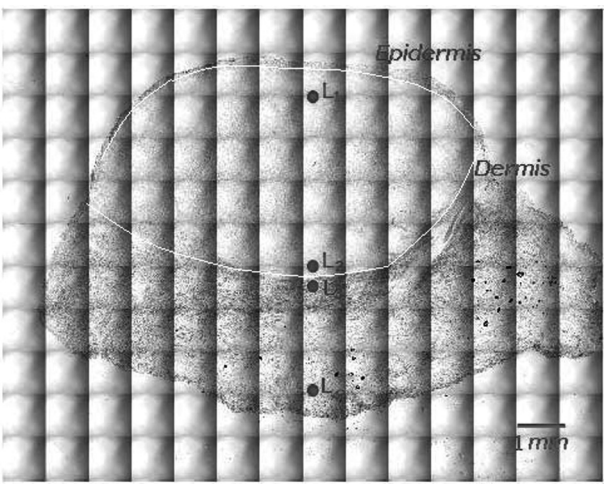

Fig. 1 The mosaic transmission mode image from the epidermis to dermis of a keloid scar tissue specimen (51-year-old patient). The white lines approximately indicate the corresponding positions of the two boundaries. Scale bar: 1 mm.

second boundary the "upper dermis," while the dermis below the second boundary is defined as the "deep dermis." Based on this definition, the average thickness of the upper dermis is 4.25 ± 0.26 mm. Locations 1 to 4 from upper dermis to deep dermis are labeled in Fig. 1 for convenient discussion of the representative morphological variation of collagen and elastin in the keloid sample.

3.2 *Multiphoton Imaging of Collagen and Elastin in Keloid Dermis Under Multichannel Mode*

Collagen and elastin are two major extracellular matrix components of human skin dermis. As a result of keloid development, keloid-derived fibroblasts result in excessive deposition and morphology changes of collagen and elastin. In this study, we operated the multiphoton microscopy under the multichannel mode. Two independent-channels from eight channels were selected to acquire 2-D and 3-D TPEF/SHG images of collagen and elastin along the central location of the keloid sample. The representative 2-D and 3-D morphological variations of collagen and elastin were shown in Figs. 2 and 3, respectively. Figure 2 shows a 2-D TPEF/SHG image around the second boundary (as illustrated in Fig. 1) across the upper dermis and the deep dermis of the keloid tissue. Figure 3 presents 3-D images of collagen and elastin with the representative morphologies at locations 1 to 4 as indicated in Fig. 1. In Fig. 3, the SHG images of collagen are shown in the first column, and the TPEF images of elastin are shown in the second column, while the superimposed SHG/TPEF images are displayed in the last column.

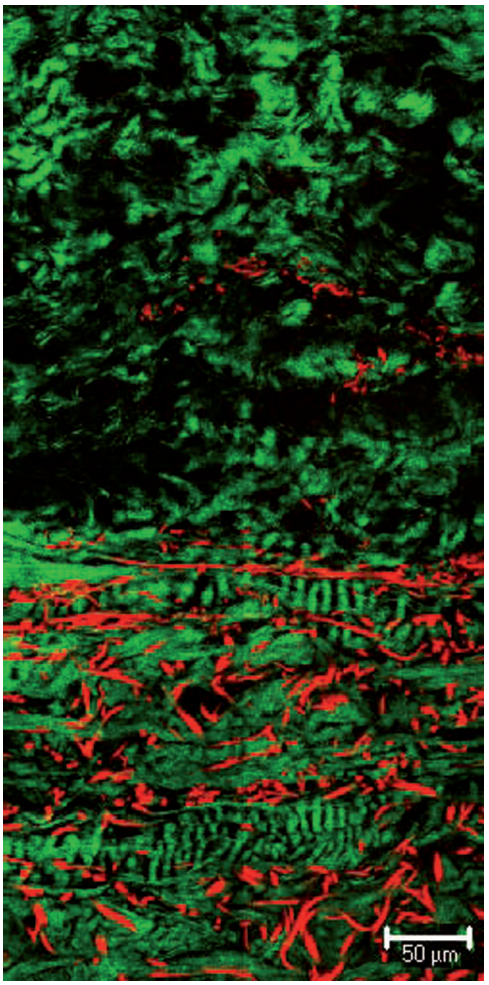

Fig. 2 The 2-D SHG/TPEF image around the boundary part across the upper dermis and the deep dermis of the keloid tissue sample. The green color-coded structure is collagen and the red color for elastin component. Scale bar: 50 μm.

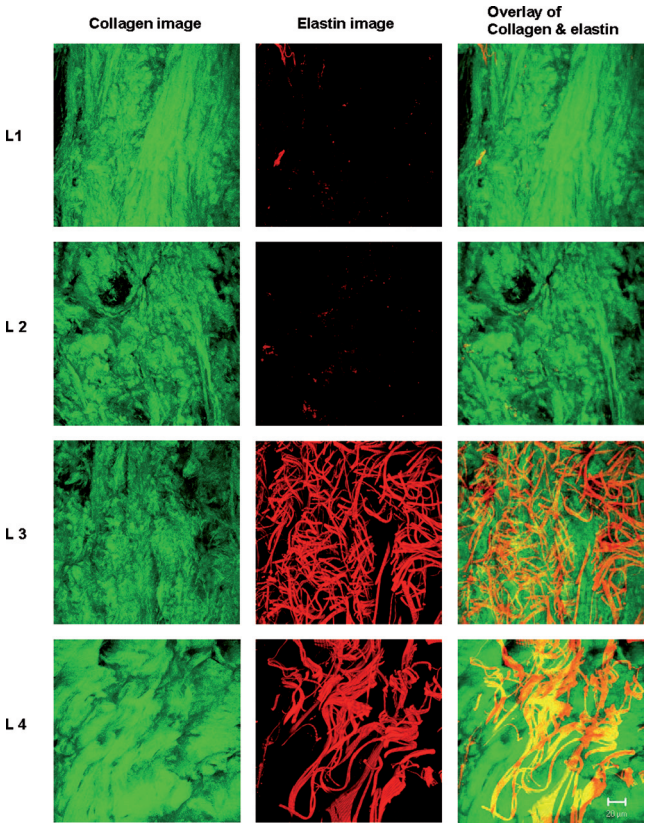

Fig. 3 The 3-D images of collagen and elastin with representative morphologies from different locations in the keloid tissue sample. The SHG images of collagen are shown in the first column, and the TPEF images of elastin are shown in the second column, while the superimposed SHG/TPEF images are displayed in the last column. Locations 1 to 4 from the upper dermis to the deep dermis have been marked in Fig. 1. All images are 146 μm×146 μm×30 μm. Scale bar: 20 μm.

As can be seen from Fig. 2, there are significant differences in the morphology and content of collagen, and elastin in the upper dermis and deep dermis of keloid tissue. In the upper dermis, elastic fibers were almost completely devoid. Very few elastic fibers in the 3-D image (Fig. 3) of elastin at locations 1 and 2 presented as irregular granules, very much like anetoderma.[18] In the deep dermis, the amount of elastic fibers was markedly increased, and the 3-D image (Fig. 3) of elastin at location 4 also showed that they have apparently accumulated together. An obvious characteristic of elastin morphology at location 3 is that each elastic fiber has many nodes. In order to quantitatively measure the distance between two nodes, we plotted the TPEF intensity profile along the selected elastic fiber. Along that line, the lowest and highest intensities are corresponding to the locations without node and with node of elastic fibers, respectively. The spacing between two nodes was determined by manually

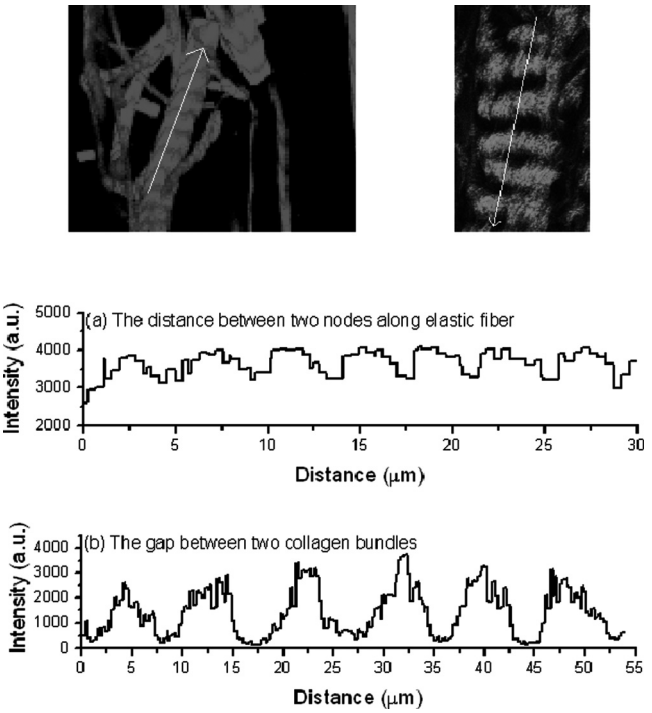

Fig. 4 The averaged distance between two nodes along elastic fiber (a) and the gap between two collagen bundles (b) in the deep dermis of keloid scar.

calculating the ratio of the selected line length to the number of peaks, as shown in Fig. 4(a). In other words, the spacing between nodes is approximately equal to the average distance of two adjacent peaks. In this work, we computed and averaged the node spacing over five selected elastic fibers. The average distance between two nodes is 4.09 ± 0.35 μm.

The morphology of collagen in keloid also showed obvious variations. Right below the boundary across the upper dermis and the deep dermis (location 3), collagen bundles apparently have regular gaps, consistent with the acellular node-like structures reported in histological study.[19] Using the same method that determined the distance between two nodes of elastic fiber, the gap between two collagen bundles was measured (Fig. 4(b)), to be 8.69 ± 0.93 μm. The appearance of a gap between two collagen bundles and nodes of elastin in keloid dermis may lead to decreasing tissue elastic properties. Far away from the boundary in the deep dermis (location 4), the regular gaps between collagen bundles disappeared. Near the top of the upper dermis (location 1), except for the similar morphology of lower part of this layer (location 2), there is a kind of special structure: the thicker and abundant collagen bundles have preferred orientation along a certain angle, which is probably toward the injury site due to their task to repair the wound.[13]

3.3 *Comparisons of Collagen and Elastin Morphology Between Normal Skin and Keloid Scar*

To better understand collagen and elastin alterations during keloid development, 3-D SHG/TPEF images of collagen and elastin were also acquired from the upper dermis and deep dermis of normal skin samples from a healthy volunteer aged 57

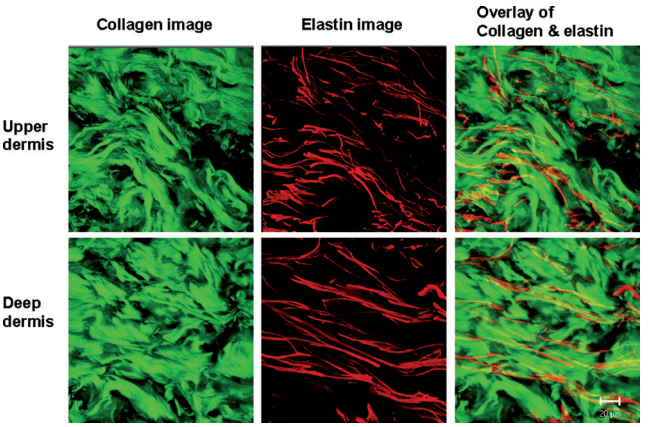

Fig. 5 The 3-D SHG/TPEF images of collagen and elastin in the upper dermis and the deep dermis of normal skin tissue sample from a healthy volunteer aged 57 years old who had no scar lesion. All images are146 μm×146 μm×30 μm. Scale bar: 20 μm.

years old who had no scar lesions. The results are shown in Fig. 5. Compared with keloid scar, morphologies and content of collagen and elastin in normal skin demonstrated apparent differences. Collagen bundles in both upper dermis and deep dermis of normal skin appear relaxed and are in an unordered arrangement. There is no regular gap between two collagen bundles, consistent with the results from histological study.[19] In keloid scar, only collagen bundles in location 4 have some similarity to normal skin collagen bundles.

The elastic fibers in both the upper dermis and the deep dermis of normal skin possess the morphology of long ropes and make elastic skin structures, very different from elastin in keloid tissue, which were fragmented, decreased in great amount with the structure of irregular granules or even disappeared in the upper dermis, but increased and showed curved or accumulated morphology in deep dermis.

3.4 *Volume Density of Collagen and Elastin in Normal Skin and Keloid Scar*

The volume density of collagen and elastin can well reflect their excessive depositions produced by keloid-derived fibroblast during the development of keloid. The volume density parameter was calculated using the quantitative analysis method presented in Sec. 2. Figure 6 compared the volume density of collagen and elastin between normal skin and keloid scar. In the upper dermis, volume density of collagen in location 2 of keloid tissue (close to the boundary across upper dermis and deep dermis) was a little bit lower than that of the normal skin, but this parameter in location 1 of keloid tissue (far from the upper dermis/deep dermis boundary) was higher than that of the normal skin. In the deep dermis, similar trends occurred. Location 3 in keloid tissue showed lower collagen volume density than normal skin, while location 4 showed higher collagen volume density than normal skin.

For the elastin component in the upper dermis, its volume density in normal skin was much higher than that in locations 1 and 2 of keloid tissue. In the deep dermis, this parameter in normal skin was lower than that of keloid scar (for both locations 3 and 4). The observation of excessive elastin production in

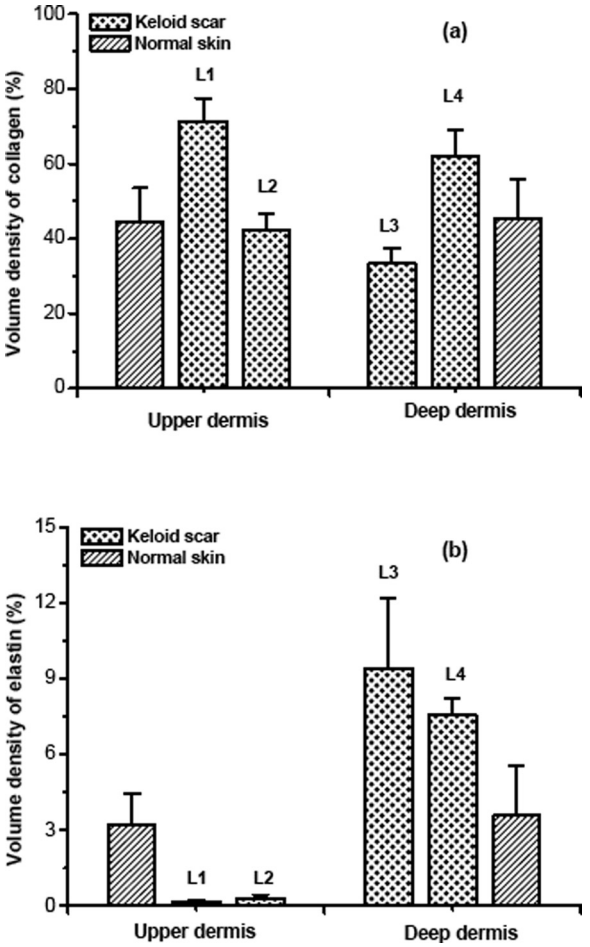

Fig. 6 The volume density of collagen (a) and elastin (b) in the upper dermis and the deep dermis of normal skin and keloid scar.

the deep dermis of keloid is consistent with the experimental results obtained using immunohistochemical and stereological techniques.[6] In summary, compared to normal skin the volume density of collagen and elastin in the deep dermis of keloid tissue both have increasing tendency, while in the upper dermis of keloid tissue only collagen volume density is increased, whereas the elastin content is greatly reduced.

4 Discussion

In this study, the morphology and quantity of collagen and elastin in keloid scar were imaged and quantitatively analyzed and compared with normal skin. Our results showed that these two extracellular matrix components synthesized by keloid-derived fibroblast have an apparently different behavior and characteristics in the upper dermis and deep dermis. In the deep dermis of keloid scar, elastic fibers showed node structure and became curved and even aggregated together, while collagen showed obvious regular gaps between adjacent bundles. In the upper dermis, collagen bundles aligned in a preferred direction, while elastin showed as sparse irregular granules. The increase of both elastin and collagen contents in the deep dermis whereas increase of collagen and the sharp decrease of elastin in the upper dermis of keloid scar is an interesting finding. This suggests the possibility that the keloid-derived abnormal fibroblast synthesized both collagen and elastin excessively at the beginning of keloid formation. However, after a certain time point during the scar development (as indicated by the second boundary in Fig. 1 and different collagen and elastin morphology and quantity across this boundary), keloid-derived fibroblasts produced mostly collagen and very little elastin. This may be the underlying reasons that most previous investigations only revealed excessive deposition of collagen[16,20] and rarely reported alterations of elastin in the formation of keloid scar.[6,21]

Our study has also demonstrated the great capability and advantages of using multiphoton microscopy for assessing the morphology and quantity variations of collagen and elastin in a keloid scar. Recent technical advancement on compact multiphoton microscopy has made *in vivo* multiphoton imaging of skin tissue a practical possibility.[9,11] This technology, if used *in vivo* for tracking the development of keloid and for assessing treatment responses, will greatly improve the basic understanding and management of this disease.

Acknowledgments

The work was supported by the Canadian Institutes of Health Research/National Natural Science Foundation of China International Scientific Exchange Program (No. 60711120031), the National Natural Science Foundation of China (Grant Nos. 60908043 and 30970783), the Program for New Century Excellent Talents in University (NCET-07–0191), and the Natural Science Funds for Distinguished Young Scholar in Fujian Province (2009J06031).

References

1. B. S. Atiyeh, M. Costagliola, and S. N. Hayek, "Keloid or hypertrophic scar: the controversy: Review of the literature," *Ann. Plast. Surg.* **54**, 676–680 (2005).
2. P. D. Butler, M. T. Longaker, and G. P. Yang, "Current progress in keloid research and treatment," *J. Am. Coll. Surg.* **206**, 731–741 (2008).
3. M. B. Brewer, A. T. Yeh, B. Torkian, C. H. Sun, B. J. Tromberg, and B. J. Wong, "Multiphoton imaging of excised normal skin and keloid scar: Preliminary investigations," *Proc. SPIE* **5312**, 204–208 (2004).
4. B. Hochman, F. X. Nahas, C. S. Sobral, V. Arias, R. F. Locali, Y. Juliano, and L. M. Ferreira, "Nerve fibres: A possible role in keloid pathogenesis," *Br. J. Dermatol.* **158**, 651–652 (2008).
5. T. S. Alster and E. L. Tanzi, "Hypertrophic scars and keloids: Etiology and management," *Am. J. Clin. Dermatol.* **4**, 235–243 (2003).
6. T. P. Amadeu, A. S. Braune, L. C. Porto, A. Desmoulière, and A. M. A. Costa, "Fibrillin-1 and elastin are differentially expressed in hypertrophic scars and keloids," *Wound Repair Regen.* **12**, 169–174 (2004).
7. H. P. Ehrlich, A. Desmoulière, R. F. Diegelmann, I. K. Cohen, C. C. Compton, W. L. Garner, Y. Kapanci, and G. Gabbiani, "Morphological and immunochemical differences between keloid and hypertrophic scar," *Am. J. Pathol.* **145**, 105–113 (1994).
8. S. M. Zhuo, J. X. Chen, B. Y Yu, X. S. Jiang, T Luo, Q. G. Liu, R. Chen, and S. S. Xie, "Nonlinear optical microscopy of the bronchus," *J. Biomed. Opt.* **13**, 054024 (2008).
9. M. J. Koehler, K. König, P. Elsner, R. Bückle, and M. Kaatz, "*In vivo* assessment of human skin aging by multiphoton laser scanning tomography," *Opt. Lett.* **31**, 2879–2881 (2006).
10. S. J. Lin, S. H. Jee, and C. Y. Dong, "Multiphoton microscopy: A new paradigm in dermatological imaging" *Eur. J. Dermatol.* **17** 361–366 (2007).
11. M. J. Koehler, S. Hahn, A. Preller, P. Elsner, M. Ziemer, A. Bauer, K. König, R. Bückle, J. W. Fluhr, and M. Kaatz, "Morphological skin ageing criteria by multiphoton laser scanning tomography: Non-invasive *in vivo* scoring of the dermal fibre network," *Exp. Dermatol.* **17**, 519–523 (2008).

12. F. A. Navarro, P. T. C. So, R. Nirmalan, N. Kropf, F. Sakaguchi, C. S. Park, H. B. Lee, and D. P. Orgill, "Two-photon confocal microscopy: A nondestructive method for studying wound healing," *Plast. Reconstr. Surg.* **114**, 121–128 (2004).
13. I. Riemann, A. Ehlers, R. LeHarzic, S. Martin, A. Reif, and K. König, "*In vivo* multiphoton tomography of skin during wound healing and scar formation," *Proc. SPIE* **6442**, 644226 (2007).
14. B. A. Torkian, A. T. Yeh, R. Engel, C. H. Sun, B. J. Tromberg, and B. J. F. Wong, "Modeling aberrant wound healing using tissue-engineered skin constructs and multiphoton microscopy," *Arch. Facial. Plast. Surg.* **6**, 180–187 (2007).
15. G. N. Chen, J. X. Chen, S. M. Zhuo, S. Y. Xiong, H. S. Zeng, X. S. Jiang, R. Chen, and S. S. Xie, "Nonlinear spectral imaging of human hypertrophic scar based on two-photon excited fluorescence and second-harmonic generation," *Br. J. Dermatol.* **161**, 48–55 (2009).
16. V. D. Costa, R. Wei, R. Lim, C. H. Sun, J. J. Brown, and B. J. F. Wong, "Nondestructive imaging of live human keloid and facial tissue using multiphoton microscopy," *Arch. Facial Plast. Surg.* **10**, 38–43 (2008).
17. A. S. Elkady, "Scanning transmitted and reflected light microscopy: A novel microscopy for visualizing biomaterials at interfaces," *Micron.* **38**, 848–853 (2007).
18. A. I. Oikarinen, R. Palatsi, G. E. Adomian, H. Oikarinen, J. G. Clark, and J. Uitto, "Anetoderma: Biochemical and ultrastructural demonstration of an elastin defect in the skin of three patients," *J. Am. Acad. Dermatol.* **11**, 64–72 (1984).
19. T. L. Tuan, and L. S. Nichter, "The molecular basis of keloid and hypertrophic scar formation," *Mol. Med. Today.* **4**, 19–24 (1998).
20. P. P. M. Zuijlen, J. J. B. Ruurda, H. A. Veen, J. Marle, A. J. M. Trier, F. Groenevelt, R. W. Kreis, and E. Middelkoop, "Collagen morphology in human skin and scar tissue: No adaptations in response to mechanical loading at joints," *Burns* **29**, 423–431 (2003).
21. N. V. Kamath, A. Ormsby, W. F. Bergfeld, and N. S. House, "A light microscopic and immunohistochemical evaluation of scars," *J. Cutan. Pathol.* **29**, 27–32 (2002).